INTERNATIONAL JOURNAL FOR NUMERICAL METHODS IN FLUIDS, VOL. 19, 479–491 (1994)

NUMERICAL INVESTIGATION OF LEADING EDGE SEPARATED FLOW OVER CRANKED WINGS USING A VORTEX LATTICE MODEL

G. BANDYOPADHYAY

Aerospace Engineering Department, Indian Institute of Technology, Kharagpur 721302, India

SUMMARY

Numerical models based on the vortex lattice concept using free vortex lines have been developed for the calculation of separated flow about cranked wings. Various separated flow models are developed assuming the flow to be separated along the leading edges of (i) the inner wing, (ii) the entire wing and (iii) the inner wing and the outboard part of the outer wing. To illustrate the effects of separation, attached flow solutions are also obtained. Results are compared with available experimental results. Agreement with separated flow solutions is usually good except at very high incidence.

KEY WORDS Cranked wings Strake Separation Free vortex Iteration

1. INTRODUCTION

Cranked wing planforms have been studied in various forms over many years. This planform, where the inner wing has a large chord and a higher angle of sweep of the leading edge than the outer parts of the wing, was originally proposed with the objective of achievng high isobar sweep in the middle part of the wing at high speeds and improving the tip-stalling behaviour at low speeds.[1] However, the disadvantage associated with such planforms is the non-uniform spanwise load distribution. To obtain a satisfactory overall design, various means of modifying the thickness, camber and twist along the span are usually adopted.

An alternative approach to cranked wing design, proposed by Kuchemann,[2] is to use a thin inner wing with a sharp edge to make the flow separate from the leading edge of the inner wing. The use of such a sharp inner wing or strake then provides a combination of leading edge separated flow with a coiled vortex sheet on the inner part and attached flow on the outer part of the same wing. The main advantage of the combined flow on such a straked configuration is observed in an enhanced lift and an extension of the lift curve through the stall. This extension of the linear characteristics is due to a delay of the bubble-type separation from the wing surface, resulting in a reduction of separation drag.

Although more lift is generated in the inner region of the wing by such partial span separation, the spanwise load distribution is still not uniform. An attempt can be made to even out the load distribution, at least partially, by maintaining the lift in the outer region near the tip. This is possible by making the leading edge of the entire outer wing also sharp (full span separation) or at least making the outboard part of the outer wing sharp (mixed span separation).

In the first case leading edge vortex sheets are produced along the leading edges of both the inner and outer wings. Experimental observations[3,4] on such configurations, termed double-delta

CCC 0271–2091/94/180479–13

Received March 1991
Revised February 1994

configurations, reveal the presence of two leading edge vortex systems at low incidence, one originating from the apex of the inner wing and the other from the leading edge breakpoint. The two vortex systems merge at higher incidence to form a single vortex.

In the second case there is again a combination of vortex flows and attached flows. On such a wing with multiflow systems there will be flow separation along the leading edge of the outboard part of the outer wing, i.e. near the wing tip. At all incidences the flow field on such a wing is characterized by the presence of two leading edge vortex systems. In the case of either full separation or mixed separation an enhanced lift is expected in comparison with the partial span separation case, since more lift is generated in the outer wing region near the tip.

Numerous experimental studies[3–8] have been conducted over the past two decades on cranked wings involving leading edge flow separation. However, the availability of theoretical methods for the analysis of separated flow about cranked wings is not so common.

For straight delta wings methods based on the slender body approximation were developed by Brown and Michael,[9] Mangler and Smith[10] and Smith.[11] Later a variety of vortex methods were developed in which separation is modelled by streamwise vortex segments.[12–15] To improve the accuracy of prediction, particularly at high angles of attack, vortex methods have been developed in which separation is represented by vortex elements.[16–20] The most comprehensive method in the second category is perhaps the one developed by Johnson *et al.*[19,20] using a higher-order panel method in which the wing is represented by quadratic doublet and linear source distributions while the rolled-up vortex sheet and the wake are represented by a quadratic doublet only. Reviews of various vortex methods are given in References 21–23.

For the strake configuration the main problem in theoretical modelling within the context of vortex methods seems to be representing the vortex field properly as it passes over the main wing. A technique termed the 'hybrid method' has been developed by Jepps[24] which combines a slender body separated flow method[9] with a three-dimensional vortex lattice model[25] for attached flow to provide a solution to the completely separated flow in an iterative manner. A simplified mathematical model has been developed by Chakrabarty and Basu[26] in which the slender wing theory[9] is used for the separated flow on the strake and the upwash field from this is fed into the vortex lattice theory[25] on the main wing, assuming that the separation vortices pass over the main wing in the chordal direction.

For double-delta configuration a two-dimensional discrete vortex model[27] has been developed in which the separated free shear layer is replaced by a number of two-dimensional point vortices. The numerical solution using this model shows two leading edge vortices separated from each other at small incidence but merging to form a bigger vortex as the angle of attack is increased.

The various vortex methods developed for calculating leading edge separated flow can be classified into three broad categories depending on the wing discretization used, i.e. conical, rectangular or streamwise panelling. Conical panelling is used by Almosnino,[14] Johnson *et al.*[19] and Jepps,[24] rectangular panelling is used by Kandil *et al.*,[12] Rechbach,[13] Levin and Katz[16] and Katz,[17] while streamwise panelling is used by Bandyopadhyay.[15] Among these different discretization schemes used, conical panelling can be applied only to delta planforms, while rectangular panelling is more flexible and is used for delta, rectangular and untapered swept configurations. Streamwise panelling is perhaps the most versatile and can be applied to an arbitrary planform.

It may be worth mentioning here that a more appropriate calculation of leading edge separated flows can be made with Euler and Navier–Stokes solvers,[28–30] which are in principle capable of capturing vorticity at a sharp edge or at a smooth edge. However, these codes require a large grid, resulting in a large computer memory and a long computing time even for simple configurations. To simulate partial span, full span and mixed span separations over a cranked wing, it seems that an extremely large grid will be necessary. Vortex methods, on the other hand, are less time-consuming and are therefore well suited for preliminary analysis of such separated flows.

In this paper an attempt has been made to develop mathematical models for cranked wing configurations in incompressible inviscid flow, taking into account the effect of partial span, full span and mixed span separations. The method is based on the vortex lattice concept using free vortex segments and is an extension of the earlier method[15] developed for calculating separated flow about delta wings at incidence and sideslip. The wing discretization scheme used in the present approach is based on streamwise panelling[15] because of its wider applicability to arbitrary planforms. The numerical solutions obtained are compared with available experimental results.[3,6]

2. MATHEMATICAL MODEL

2.1. Attached flow model

To illustrate the difference from the separated flow models, the attached flow (AF) model based on the well-known vortex lattice theory[25] is described briefly. The wing chordal surface is discretized into a large number of quadrilateral panels, on each of which a horseshoe vortex is introduced (Figure 1). The strength of the horseshoe vortex is constant for each panel but varies from panel to panel. Satisfying the boundary condition of zero normal velocity at all collocation points results in a system of linear algebraic equations which can be written in matrix form as

$$[A_{ji}]\,\{\Gamma_i\} = -U_\infty\{\alpha\}, \tag{1}$$

where A_{ji} is the influence coefficient matrix, Γ_i is the strength of the horseshoe vortex on the ith panel, U_∞ is the freestream speed and α is the angle of incidence.

In this model of the flow only bound vortices carry lift. Once the solution of the system of

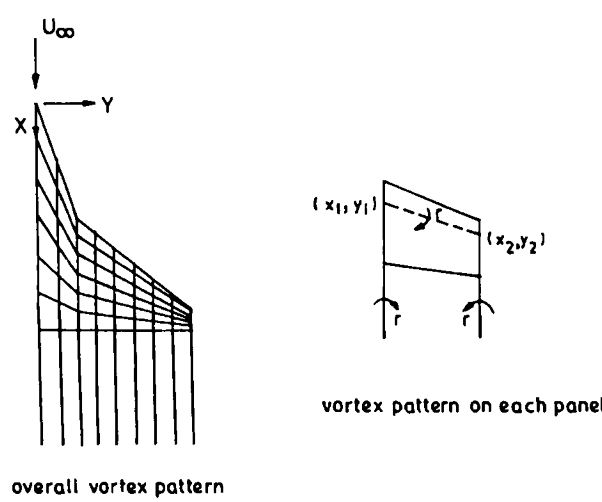

Figure 1. Attached flow model

equations (1) is obtained by any standard method, the loading on each bound vortex is given by

$$F_z = \rho U_\infty \Gamma \Delta y, \tag{2}$$

where Δy is the spanwise length component of the bound vortex segment. The overall lift coefficient can be obtained by numerical integration as

$$c_L = \frac{1}{\frac{1}{2}\rho U_\infty^2 S} \sum_{i=1}^{NM} \Delta F_z = \frac{2}{U_\infty S} \sum_{i=1}^{NM} \Gamma \Delta y, \tag{3}$$

where N and M are the numbers of divisions in the chordwise and the spanwise direction respectively, S is the wing area, c is the local chord, b is the span of the wing and (x_1, y_1) and (x_2, y_2) are the endpoints of each bound vortex segment (Figure 1).

The pitching moment and the spanwise load distribution can be calculated similarly by numerical integration.[25]

2.2 Separated flow models

The separated flow models differ primarily from the attached flow model in the formation of free vortex sheets along sharp edges where separation occurs. To simulate separation along sharp edges, 'separation panels' with a vortex pattern (ABCDEF) different from the horseshoe vortex (ABCD) are placed adjacent to the leading edge where it is sharp, as shown in Figure 2. In the full span separation (FSS) model, for the case where the flow is separating along the leading edges of both the inner and outer wings, separation panels are placed along the entire leading edge. For the partial span separation (PSS) case separation panels are placed along the leading edge of the inner wing only. Similarly, for the case of mixed span separation (MSS) these panels are placed along the leading edge where it is sharp, i.e. along the leading edge of the inner wing and the outboard part of the outer wing.

On each separation panel the horseshoe vortex pattern is modified by suppressing one of the trailing vortices (AB or CD) as shown in Figure 2. For reasons of symmetry, the right trailing vortex (CD) is suppressed for starboard panels and the left trailing vortex (AB) for port panels. Instead of taking this trailing vortex downwards to infinity downstream, it is taken upwards until it meets the leading edge at D and is then continued into the fluid to form a free vortex line (DEF). Each of these free vortex lines is composed of a series of straight line segments, except for the last segment (EF) which is semi-infinite and extends downstream. The direction of any finite segment is unknown and is determined as a part of the solution, but the last semi-infinite segment is aligned with the freestream direction.

Since the strengths and positions of the free vortex segments are unknown, an iterative procedure is set up for the solution. To start with, the initial direction of the free vortex segments is taken as the mean flow direction as argued by Kuchemann,[31] i.e. at an angle $\alpha/2$ to the mainstream. With this prescribed wake shape the unknown vortex strengths are obtained by satisfying the flow tangency condition. The set of linear algebraic equations in this case may be given by

$$[B_{ji}]\,\{\Gamma_i\} = -U_\infty\{\sin\alpha\}. \tag{4}$$

In the subsequent iterative procedure the directions of all vortex segments in a free vortex line are changed one-by-one in the downstream direction to make each segment parallel to the velocity computed at its midpoint, starting at the separation point. In adjusting the downstream

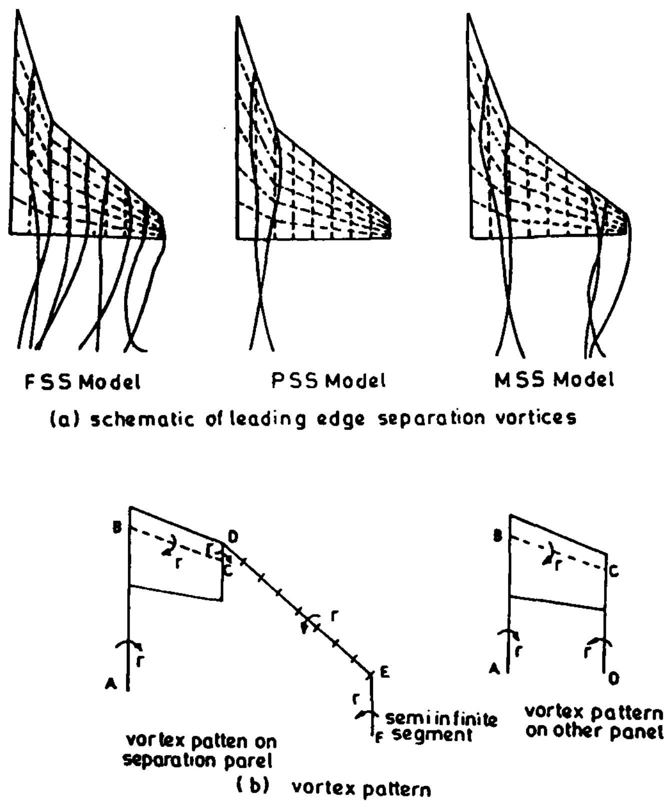

Figure 2. Flow models with leading edge separation

endpoint of each segment in this way, an inner iteration is necessary to repeat the process, since the final positions of the segment midpoints do not coincide with the positions when the velocities were calculated at them.

With the wake fixed in its new position, the influence coefficient matrix B_{ji} is recalculated and new vortex strengths are redetermined from the flow tangency condition, equation (4). The iteration is terminated when the change in lift coefficient is below 2%. This is usually achieved within nine iterations.

Once the convergence is achieved, the overall lift coefficient can be calculated by numerical integration as before. However, in the separated flow models both 'bound' and 'trailing' vortices (except the free vortex segments) carry lift.

The load carried by each 'bound' vortex segment in each panel is obtained as[25]

$$F_x = -\rho\Gamma(U_\infty \sin\alpha + w)\Delta y, \tag{5}$$

$$F_z = \rho\Gamma(U_\infty \cos\alpha + u)\Delta y - v\Delta x, \tag{6}$$

where Δx and Δy are the length components of the bound vortex segment in the chordal and the spanwise direction respectively and u, v and w are the perturbation velocity components calculated at the midpoint of the bound vortex segment.

In calculating the load carried by the trailing vortices, the length of the trailing vortex in each panel is taken as extending from the quarter-chord of the panel to the quarter-chord of the adjacent panel in the same chordwise strip in the chordal direction (i.e. $\Delta y = 0$) and the perturbation velocity components are calculated at the midpoint of this length. The load carried by each trailing vortex segment is given by

$$F_x = 0, \tag{7}$$

$$F_z = -\rho \Gamma v \Delta x. \tag{8}$$

Once the total load on each panel is computed by adding the load carried by the bound and two trailing vortices (one trailing vortex for separation panels), the resulting lift coefficient can be obtained by numerical integration as

$$C_L = \frac{1}{\frac{1}{2}\rho U_\infty^2 S} \sum_{i=1}^{NM} (\Delta F_z \cos\alpha - \Delta F_x \sin\alpha). \tag{9}$$

Since there is no suction force acting on the sharp leading edges, the resultant air force is nearly normal to the chordal plane of the wing and the induced drag coefficient may be obtained from

$$C_{D_i} = C_L \tan\alpha. \tag{10}$$

The pitching moment and spanwise load distribution can be calculated by similar numerical integration.[25]

3. COMPUTATIONAL DETAILS

Computer programmes have been developed in FORTRAN IV for the attached and various versions of the separated flow models. In all the separated flow models the length of each free vortex line (excluding the last semi-infinite segment) is taken as twice the root chord so that it extends at least one chord downstream of the wing trailing edge. Each of these vortex lines is divided into 20 straight line segments. With fewer divisions, i.e. with longer segments, the numerical inaccuracy in calculating the direction cosines of these segments increases and they may not remain non-intersecting. Safeguards are necessary in the calculation of induced velocities, particularly for larger spanwise divisions of the wing surface, since the free vortices may come too close to each other (or to a wing collocation point, especially at low angles of attack). A number of regularizing schemes have been developed to overcome the problem due to singularity of the velocity field kernel, all of which are dependent on the choice of a cut-off length.[14,21,22,32] In the present approach the cut-off length proposed by Almosnino[14] has been used. This cut-off length r^*, inside which solid body rotation is assumed, is given by Almosnino[14] as

$$r^* = \left(\frac{\Gamma \Delta x(\cos\beta + \cos\gamma)}{4\pi U_\infty}\right)^{1/2}, \tag{11}$$

where Γ is the strength of the influencing vortex segment, Δx is the length of the vortex segment at the midpoint of which the velocity is calculated, and β and γ are the geometric angles at the endpoints of the vortex segment.

Results are obtained with an optimum of 96 panels ($M = 12$, $N = 8$). The programmes are run on a Horizon III minicomputer.

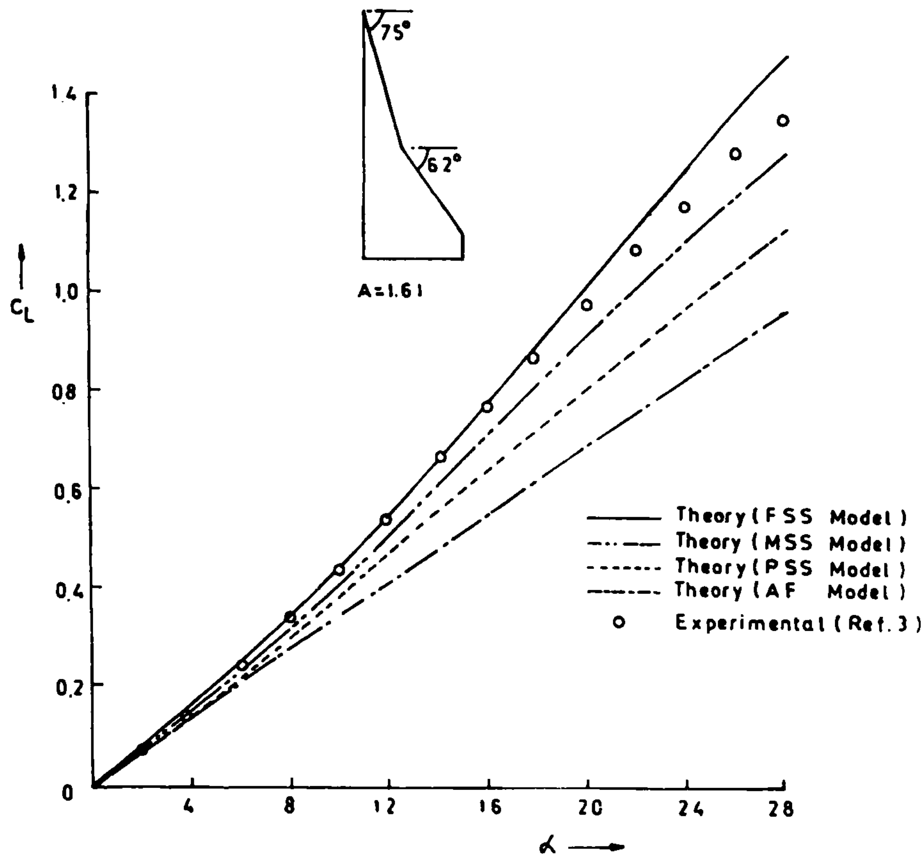

Figure 3. Variation in lift with angle of attack

4. RESULTS AND DISCUSSION

Results are obtained by the three different separated flow models for a 75°/62° double-delta configuration and are compared with experimental results[3] in Figure 3. To illustrate the effect of flow separation, the attached flow solution is also plotted in the same figure. The comparison with experimental results is reasonably good for the FSS model except at high incidence. The PSS and MSS models both underpredict the lift, as expected. The discrepancy at higher angles of attack is presumably due to bubble-type separation from the wing surface and associated vortex breakdown effects, the influence of which is not taken into account in the numerical model.

To illustrate the advantage of adding a thin inner wing to the basic 62° cropped delta planform, results for the 62° delta configuration are obtained and compared with the 75°/62° configuration in Figure 4. In order to compare directly, the parameter C_L/A (where A is the aspect ratio) rather than C_L is used. The comparison in this form shows that both configurations develop the same amount of lift up to an angle of incidence of 4°. Beyond 4° the 75°/62° configuration develops greater lift. The other advantage is seen in the extension of the linearity of the lift curve slope, indicating delayed stall.

The separation of vortices from the entire leading edge of the 75°/62° configuration is shown

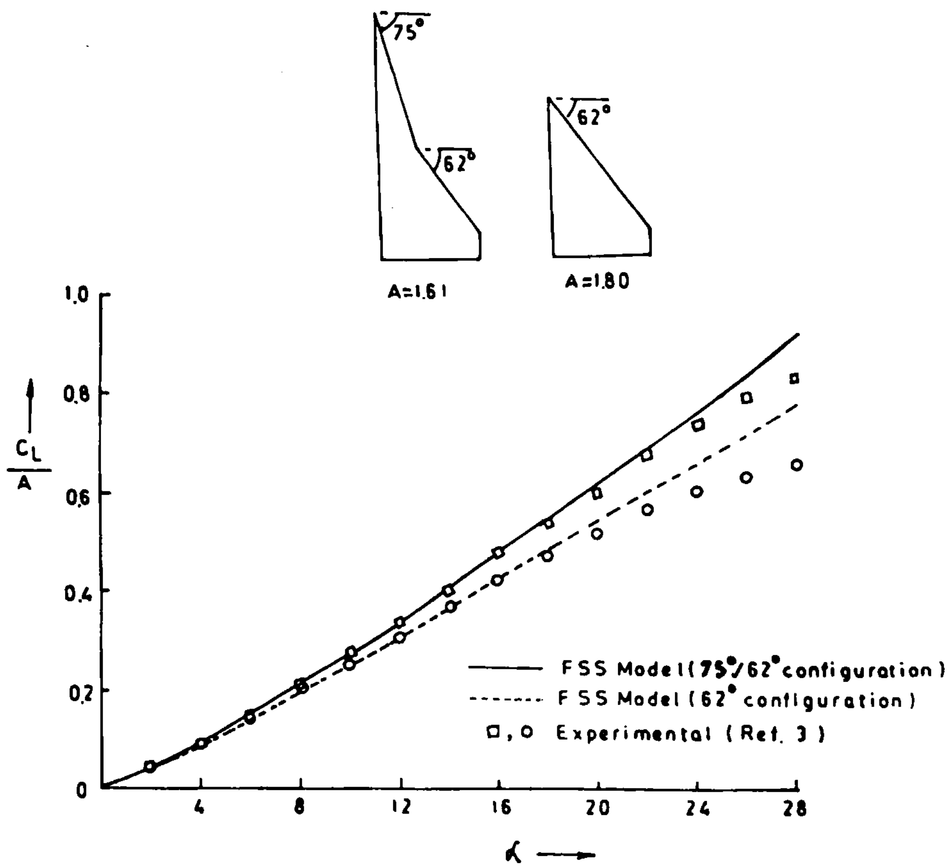

Figure 4. Variation in C_L/A with angle of attack

in Figure 5 at 12° incidence. The arrangement of vortex lines calculated by the FSS model using an 8 × 12 lattice is shown in three views. For clarity, vortex lines issuing from the trailing edge are omitted in this figure. Rolling up of the vorticity resulting in the formation of two rolled-up vortex sheets is not so pronounced in this figure, presumably owing to the small number of spanwise divisions. The lift coefficients obtained by the attached and different separated flow models at this angle of incidence are also shown in this figure.

An explanation of the difference in lift coefficients calculated by the different separated models follows from the spanwise load distribution shown in Figure 6. The PSS model shows a suction peak near the strake tip, indicating considerable lift generation in the inner region of the wing due to vortices separating from the inner wing leading edge. A further enhancement in lift is achieved with the FSS model, since more lift is generated in the inner as well as in the outer swept part, as evidenced by two distinct suction peaks. The spanwise load distribution obtained by the MSS model is somewhat similar to that obtained by the PSS model. The effect of the second primary vortex originating from the discontinuity in the leading edge shape at the middle of the outer wing is not so pronounced. The second vortex may be made stronger and more lift in the outer part may perhaps be generated by introducing a second kink in the planform shape

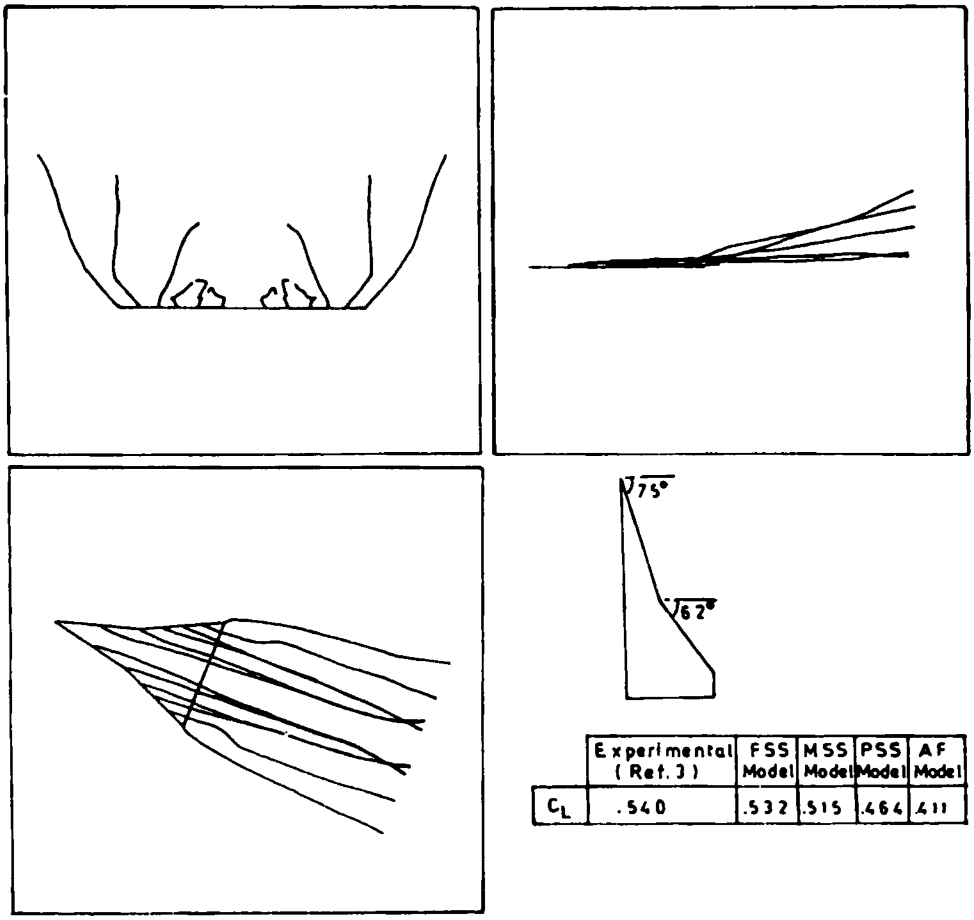

	Experimental (Ref. 3)	FSS Model	MSS Model	PSS Model	AF Model
C_L	.540	.532	.515	.464	.411

Figure 5. Flow pattern and C_L-values at $\alpha = 12°$

from this point of discontinuity, with the sweep of the outboard part as high as the sweep of the inner wing.

The moment characteristics (Figure 7) exhibit a non-linear increase in pitching moment (pitch-up) for a lift coefficient above 0.4. Comparison of the experimental data with the FSS model again shows good agreement except at high incidence. The attached flow solution is also plotted to indicate the effect of leading edge flow separation.

The induced drag data show good agreement with the calculated $C_{D_i} = C_L \tan \alpha$ (Figure 8), illustrating that the resultang force developed by a wing with leading edge separated flow is essentially a normal force.

Theoretical results are also plotted for a 77°/59° cranked configuration (Figure 9) for which experimental results are available in Reference 6. In the experimental model[6] the entire leading edge is sharp; the section of the outer wing is NACA 0003-03 and that of the inner wing is a wedge of angle 20°. The experimental results again show better agreement with the more consistent FSS model except at high incidence. However, the difference between the results obtained by the FSS and PSS models is small, presumably because of the comparatively smaller outer wing area.

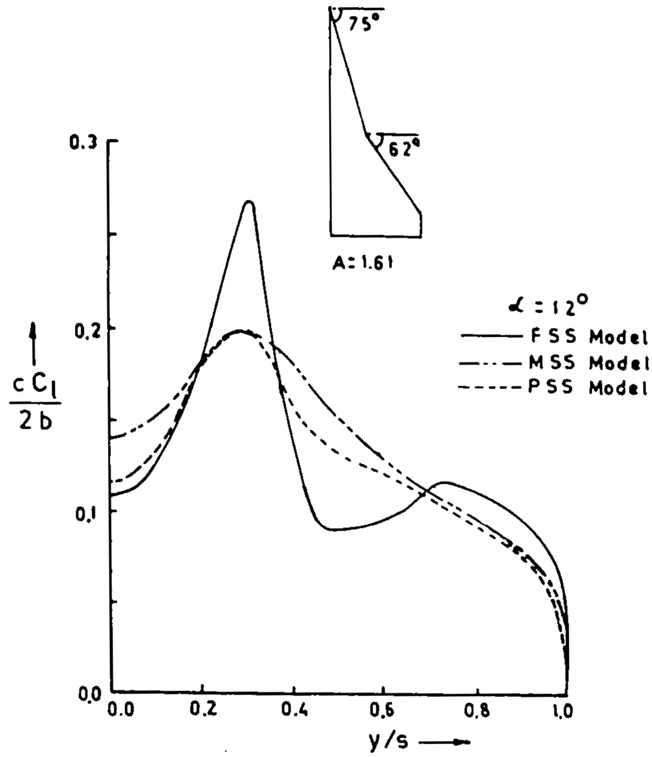

Figure 6. Spanwise load distribution

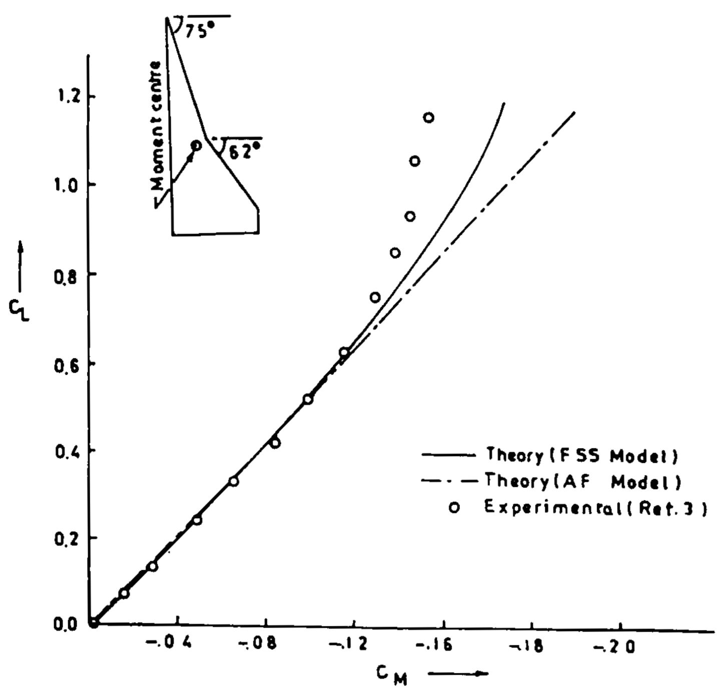

Figure 7. Variation in pitching moment with lift

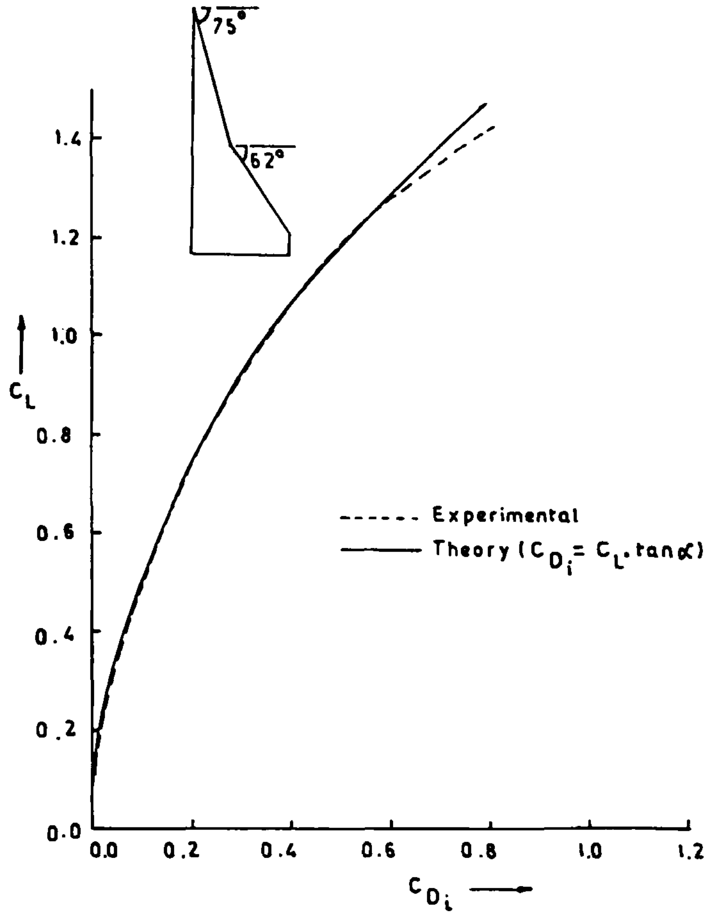

Figure 8. Variation in induced drag with lift

5. CONCLUDING REMARKS

Separated flow models have been developed for the calculation of potential flow about cranked wings with a variety of leading edge shapes. The full span separation model developed for cranked wings with an entirely sharp leading edge is capable of predicting aerodynamic forces and moments at high incidence until bubble-type separation occurs. The solutions obtained by other flow models, e.g. part span and mixed span separation models, are shown to be consistent with the aerodynamic characteristics of relevant planforms. To indicate the effects of separation, the attached flow solution is also obtained.

The numerical results presented in this paper illustrate some of the general aerodynamic characteristics of the cranked configuration with a large centre chord. If the inner wing is thin and sharp-edged, there is a combination of vortex flow and attached flow and this combined flow produces more lift in the inner region. More lift is generated in the inner as well as the outer part by making the entire leading edge sharp. However, if a thick and round-edged outer wing is necessary, a compromise may be made by introducing a discontinuity in the leading edge in the outboard part of the outer wing by making the leading edge sharp there. This will produce a combination of vortex flow and attached flow on the same wing. Such a multiflow

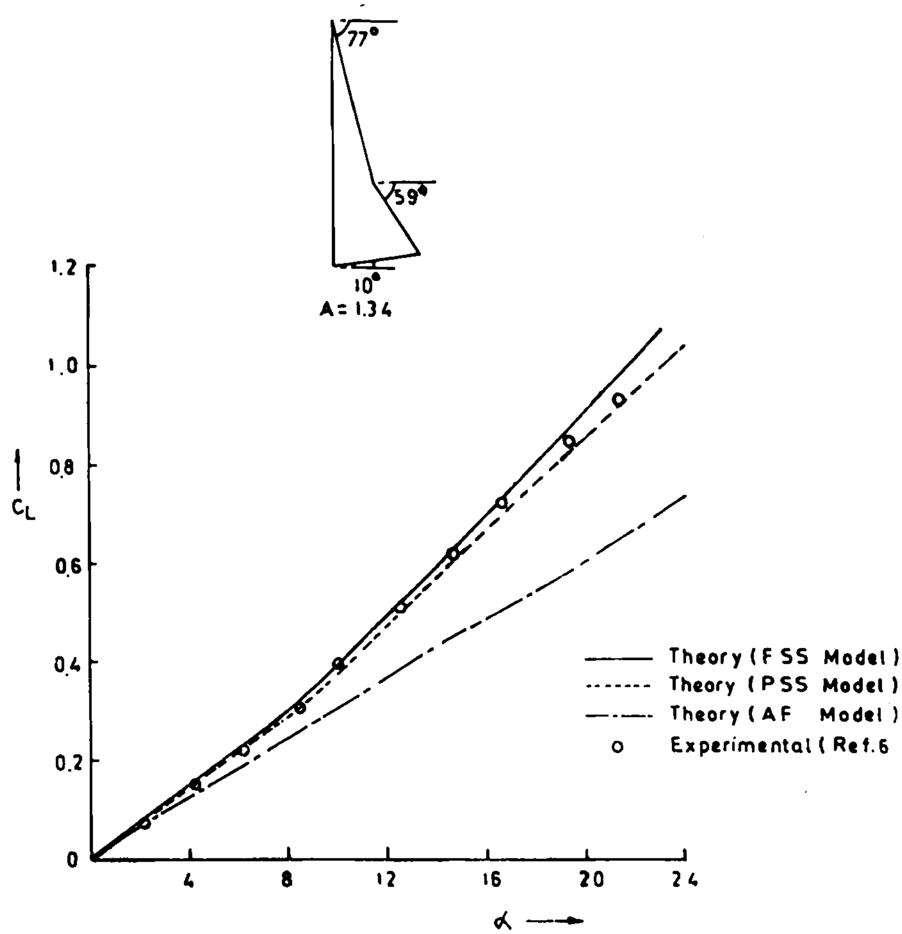

Figure 9. Variation in lift with angle of attack

design may be more efficient if a second kink is introduced at the point of discontinuity, with the sweep of the outboard part as high as the sweep of the inner wing.

REFERENCES

1. R. Hills and D. Kuchemann, 'A note on cranked sweptback wings', *RAE TN Aero 1911*, 1966.
2. D. Kuchemann, 'On the possibility of designing wings that combine vortex flows with classical aerofoil flows', *RAE TM Aero 1363*, 1971.
3. W. H. Wentz and M. C. McMahon, 'Experimental investigations of the flow field about delta and double delta wings at low speeds', *NASA CR 521*, 1966.
4. U. Brennenstuhl and D. Hummel, 'Untersuchungen über die Wirbelbildung an Flugeln mit geknickten Vorderkanten', *Z. Flugwiss. Weltraumf.*, **5**, 375–381 (1981).
5. U. Brennenstuhl, 'Experimentelle und theoretische Untersuchungen über die Wirbelbildung an Doppeldeltaflugeln', *Ph.D. Thesis*, Technische Universität Braunschweig, 1985.
6. V. R. Corsiglia and D. G. Koenig, 'Large-scale wind-tunnel tests of a low-aspect-ratio delta-winged model equipped with sharp-edged strake', *NASA TN D-3621*, 1966.
7. W. Staudacher, 'Verbesserung der Manoeverleistungen im hohen Unterschall in DLR-Mitt', *NASA TT-F-15406*, 1974.
8. G. F. Moss, 'Some UK research studies of the use of wing-body strakes on combat aircraft configurations at high angles of attack', *RAE TM Aero 1772*, 1978.

9. C. E. Brown and W. H. Michael, 'On slender delta wings with leading edge separation', *NACA TN 3430*, 1955.
10. K. W. Mangler and J. H. B. Smith, 'Calculation of the flow past a slender delta wing with leading edge separation', *RAE Rep. Aero 2593*, 1957.
11. J. H. B. Smith, 'Improved calculations of leading edge separation from slender delta wings', *RAE Tech. Rep. 66070*, 1966.
12. O. A. Kandil, D. T. Mook and A. H. Nayfeh, 'Nonlinear prediction of aerodynamic loads on lifting surfaces', *J. Aircraft*, **13**, 22–28 (1976).
13. C. Rechbach, 'Calcul instationaire des nappes tourbillonaires emises par des surfaces portantes fortment inclinées', *AIAA Paper 78-111*, 1978.
14. D. Almosnino, 'High angle of attack calculation of the subsonic vortex flow on slender bodies', *AIAA J.*, **23**, 1150–1156 (1985).
15. G. Bandyopadhyay, 'Application of a vortex lattice numerical model in the calculation of inviscid incompressible flow around delta wings', *Int. j. numer. methods fluids*, **10**, 729–740 (1990).
16. D. Levin and J. Katz, 'Vortex-lattice method for the calculation of the nonsteady separated flow over delta wings,' *J. Aircraft*, **18**, 1032–1037 (1981).
17. J. Katz, 'Lateral aerodynamics of delta wings with leading edge separation', *AIAA J.*, **22**, 323–328 (1984).
18. C. Costis and D. P. Telionis, 'Unsteady vortical wakes over a prolate spheroid', *AIAA Paper 84-0419*, 1984.
19. F. T. Johnson, P. Lu, G. W. Brune, J. A. Weber and P. E. Rubbert, 'An improved method for the prediction of completely three-dimensional aerodynamic load distributions of configurations with leading edge vortex separation', *AIAA Paper 76-417*, 1976.
20. F. T. Johnson, E. N. Tinoco, P. Lu and M. A. Epton, 'Three-dimensional flow over wings with leading edge vortex separation', *AIAA J.*, **18**, 367–380 (1980).
21. A. Leonard, 'Vortex methods for flow simulation', *J. Comput. Phys.*, **37**, 289–335 (1980).
22. A. Leonard, 'Computing three-dimensional incompressible flows with vortex filaments', *Ann. Rev. Fluid Mech.*, **17**, 523–559 (1985).
23. A. G. Parker, 'Aerodynamic characteristics of slender wings with sharp leading edges—a review', *J. Aircraft*, **13**, 161–168 (1976).
24. S. A. Jepps, 'The computation of vortex flows by panel methods', *VKI Lect. Ser. 5*, 1978.
25. P. E. Rubbert, 'Theoretical characteristics of arbitrary wings by a nonplanar vortex lattice method', *Boeing Co. Rep. D6-9244*, 1964.
26. S. K. Chakrabarty and B. C. Basu, 'Approximate analysis of strake wings at low speeds', *AIAA J.*, **17**, 432–434 (1979).
27. Xie-yuan, X. Nan and D. Guo-hua, 'Numerical simulation of rolling up of leading/trailing-edge vortex sheets for slender wings', *AIAA J.*, **27**, 1313–1318 (1989).
28. K. Fujii, S. Gavali and T. L. Holst, 'Evaluation of Navier–Stokes and Euler solutions for leading edge separation vortices', *Int. j. numer. methods fluids*, **8**, 1319–1329 (1988).
29. A. Rizzi and B. Muller, 'Large-scale viscous simulation of laminar vortex flow over a delta wing', *AIAA J.*, **27**, 833–840 (1989).
30. S. E. Rogers and D. Kwak, 'Upwind differencing scheme for the time-accurate incompressible Navier–Stokes equations', *AIAA J.*, **28**, 253–262 (1990).
31. D. Kuchemann, 'A nonlinear lifting-surface theory for wing of small aspect ratio with edge separations', *RAE Rep. Aero 2540*, 1955.
32. J. T. Beale and A. Majda, 'Vortex methods', *Math. Comput.*, **159**, 1–52 (1982).